

Cluster-scaling, chaotic order and coherence in DNA

A. Bershadskii

ICAR, P.O. Box 31155, Jerusalem 91000, Israel

Abstract

Different numerical mappings of the DNA sequences have been studied using a new cluster-scaling method and the well known spectral methods. It is shown, in particular, that the nucleotide sequences in DNA molecules have robust cluster-scaling properties. These properties are relevant to both types of nucleotide pair-bases interactions: hydrogen bonds and stacking interactions. It is shown that taking into account the cluster-scaling properties can help to improve heterogeneous models of the DNA dynamics. It is also shown that a chaotic (deterministic) order, rather than a stochastic randomness, controls the energy minima positions of the stacking interactions in the DNA sequences on large scales. The chaotic order results in a large-scale chaotic coherence between the two complementary DNA-duplex's sequences. A competition between this broad-band chaotic coherence and the resonance coherence produced by genetic code has been briefly discussed. The Arabidopsis plant genome (which is a model plant for genome analysis) and two human genes: BRCA2 and NRXN1, have been considered as examples.

1 Introduction

A DNA molecule carries information in the form of four chemical groups or nucleotide bases: adenine, cytosine, guanine, and thymine, represented by the letters A, C, G and T. The order of bases on a DNA strand is the DNA sequence. If we read along one of the two DNA-helix sides we get text like GATACA... In the double-stranded DNA, the two strands run in opposite

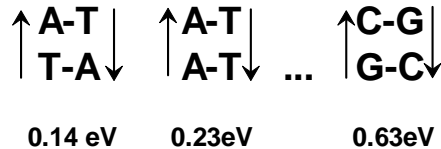


Figure 1: The stacking energies for different stacked base pairs.

directions and the bases pair up such that A always pairs with T and G always pairs with C. That is because these particular pairs fit exactly to form effective hydrogen bonds with each other. The A-T base-pair has 2 hydrogen bonds and the G-C base-pair has 3 hydrogen bonds. The G-C interaction is therefore stronger than A-T, and A-T rich regions of DNA are more prone to thermal fluctuations and to initiation sites (origin) at unwinding stage of DNA replication process. The bases are oriented perpendicular to the DNA-helix axis. Constant thermal fluctuations result in local twisting, stretching, bending, and unwinding of the double-strands. In solution DNA assumes linear configuration because it is the one of minimum energy. The helix axis of DNA in vivo is usually strongly curved because the stretched length of the human genome, for instance, is about 1 meter and this length needs to be "packaged" in order to fit in the nucleus of a cell (the diameter of the nucleus from a typical human somatic cell is about 5×10^{-6} meters). Therefore, the DNA has to be highly organized. This packaging of DNA deforms it physically, thereby increasing its energy (less stable than relaxed DNA, due to less than optimal base stacking). In this situation certain strain is relieved by supercoiling: helix bends and twists to achieve better base stacking orientation despite having too many bp/turn. The difference in A-T and G-C interactions can be used for optimizing the free energy. The base-pairs stacking energies (the main stabilizing factor in the DNA duplex, see for instance Ref. [1]) are highly dependent on the base sequence [2]. These interactions come partly from the overlap of the π electrons of the bases and partly from hydrophobic interactions. Quantum chemistry calculations give rather different energies for different stacked base pairs: Fig. 1 (cf. Ref. [3]). Therefore, certain clustering of the base-pairs can be used by nature in order to minimize the excess energy that builds up when DNA molecules are deformed during the process of packaging. The physical constraints given by the supercoiling of the DNA sequence, in particular to the positioning of nucleosomes along the sequence [4], play significant role in creating of the clustering.

Moreover, the increase in stored (potential) energy within the molecule

is then available to drive reactions such as the unwinding events that occur during DNA replication. Before replication of DNA can occur, the length of the DNA double helix about to be copied must be unwound and the two strands must be separated by breaking the hydrogen bonds that link the paired bases. The process of replication begins in the DNA molecules at thousands of sites called origins of replication. Because the location and time of initiation of origins is generally stochastic, the time to finish replication will also be a stochastic process. The random distribution of origin firing raises the random gap problem: a random distribution will lead to occasional large gaps that should take a long time to replicate. Despite this each cell in a population must complete the replication process in an accurate and timely manner (see for instance, Refs. [5],[6]). Different solutions to this problem have been suggested (see, for instance, Refs. [7],[8],[9],[10]) .

If the spacing of origins is not completely random then any regularity in the spacing of origins will tend to suppress the large gaps [7]. For instance, origins within specific clusters could be preferred to fire [11],[12]. Since a G-C base pair, with three hydrogen bonds, is expected to be harder to break than an A-T base pair with only two bonds, a clustering of these two kinds of the base-pairs can be operational in order to solve the random origin firing problem. The stacking interactions can also contribute to solution of this problem. It will be shown below that a chaotic (deterministic) order, rather than a stochastic randomness, controls the energy minima positions of the stacking interactions in the DNA sequences on large-scales. This chaotic order not only introduces a regularity into the spacing of the origins but also results in a long-range coherence between the two complimentary DNA-duplexs strands.

2 Cluster-scaling

Because of many orders of space scales involved in these processes one can expect that the clustering will exhibit scale-invariant properties (see, for instance, Ref. [13]). A cluster-scaling for stochastic systems was recently suggested in Refs. [14],[15],[16]. The genome data can be readily checked on the cluster-scaling properties in a "1 or 0" mapping. In this presentation (see, for instance Refs. [18],[23] and references therein) one should put A=1 and C=G=T=0 in an original DNA sequences to obtain an A-dominated sub-sequences (one can obtain C or G, or T-dominated sub-sequences in

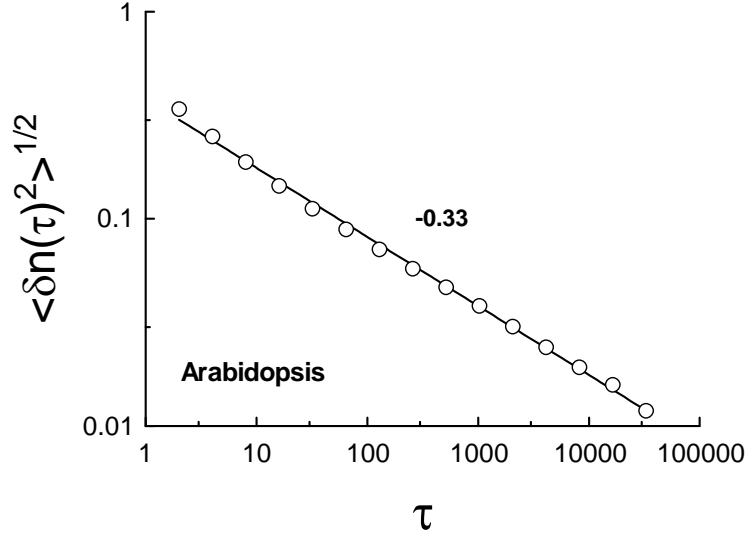


Figure 2: The standard deviation for $\delta n(\tau)$ vs τ for T-dominated sub-sequence of the Arabidopsis (in log-log scales). The straight line (the best fit) indicates the scaling law Eq. (2).

analogous way). Then, to study statistical clustering in sub-sequences $\{a_i\}$ (where $a_i=1$ or 0 and $i = 1, 2, \dots$) one should take running average:

$$n_j(\tau) = \frac{1}{\tau} \sum_{i=j}^{i=j+\tau} a_i \quad (1)$$

along the sub-sequences. For the 1 or 0 mapping this running average will present a weight of the sub-sequences in interval $[j, j + \tau]$. Following to Ref. [14] we are interested in scaling variation of the standard deviation of the running density fluctuations $\langle \delta n_j(\tau)^2 \rangle^{1/2}$ with τ

$$\langle \delta n_j(\tau)^2 \rangle^{1/2} \sim \tau^{-\alpha} \quad (2)$$

where $\langle \dots \rangle$ denotes average over the sub-sequences, $\delta n_j(\tau) = n_j(\tau) - \langle n(\tau) \rangle$. The power law, Eq. (2), corresponds to a scale-invariant (scaling) behavior.

The exponent α in Eq. (2) was called in Ref. [14] as cluster-exponent. For white noise zeros (intersections of a white noise signal with time axis) it can be derived analytically that $\alpha = 1/2$ (see Ref. [14] and references therein). This value can be considered as an upper limit (non-clustering case) for the cluster-exponent. If $0 < \alpha < 0.5$ we have a cluster-scaling situation, and the cluster-scaling is stronger for smaller values of α (see for examples Ref. [14]).

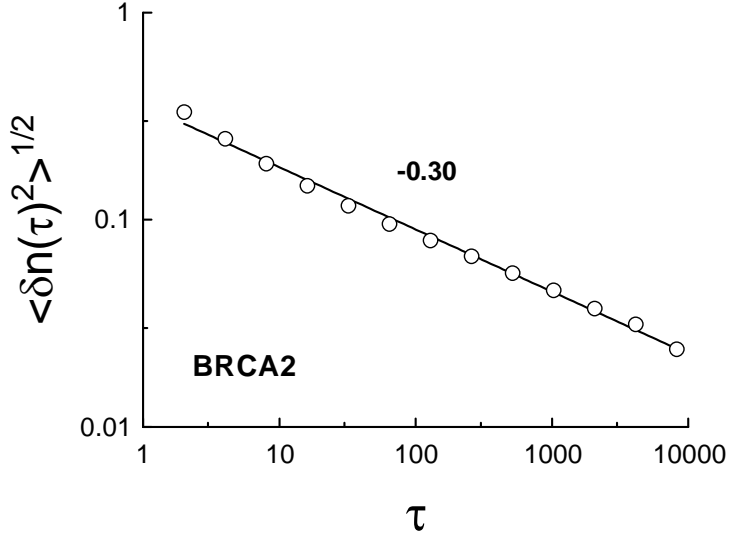


Figure 3: The standard deviation for $\delta n(\tau)$ vs τ for T-dominated subsequence of gene BRCA2 (in log-log scales). The straight line (the best fit) indicates the scaling law Eq. (2).

In this paper we will present, as an example, results obtained for the genome sequence of the flowering plant *Arabidopsis thaliana*, which is a model plant for genome analysis [17] and for two human genes BRCA2 and NRXN1.

Let us start from the *Arabidopsis*. Its genome is one of the smallest plant genomes (about 157 million base pairs and five chromosomes) that makes *Arabidopsis thaliana* useful for genetic mapping and sequencing. The most up-to-date version of the *Arabidopsis thaliana* genome is maintained by The *Arabidopsis* Information Resource (TAIR) (see, for instance, <http://www.plantgdb.org/>). The results of computations for the genome sequences associated with the *Arabidopsis* are shown in figure 2. We show in Fig. 2 results for the T-dominated sub-sequence, whereas the results for A, C, and G-dominated sub-sequences are similar to those shown in the Fig. 2. The Fig. 2 shows (in the log-log scales) dependence of the standard deviation of the running density fluctuations $\langle \delta n(\tau)^2 \rangle^{1/2}$ on τ for the T-dominated subsequence. The straight line is drawn in this figure to indicate the scaling (2). The slope of this straight line provides us with the cluster-exponent $\alpha = 0.33 \pm 0.02$. The results of computations for the genome sequences associated with genes: BRCA2 and NRXN1, are shown in figures 3 and

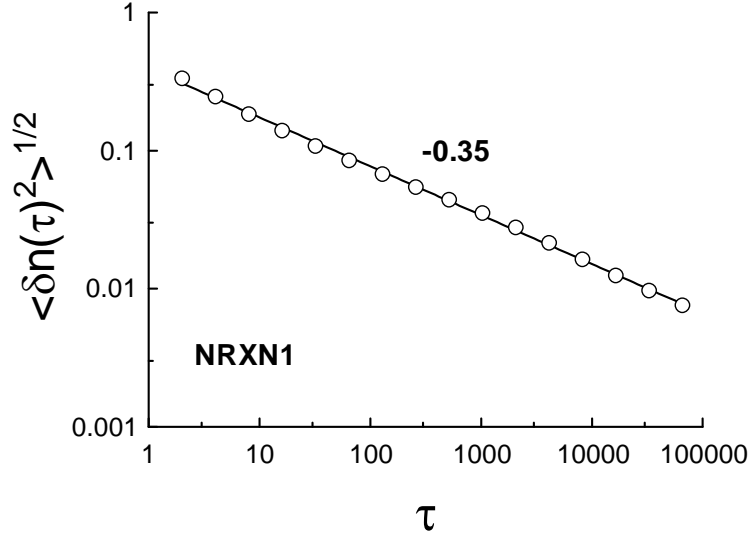


Figure 4: The standard deviation for $\delta n(\tau)$ vs τ for T-dominated subsequence of gene NRXN1 (in log-log scales). The straight line (the best fit) indicates the scaling law Eq. (2).

4 respectively (the full set of the genome sequences can be found in site: <http://www.ncbi.nlm.nih.gov>). Molecular location of gene BRCA2 on chromosome 13: base pairs 32,889,616 to 32,973,808). BRCA2 gene helps prevent cells from growing and dividing too rapidly or in an uncontrolled way. By helping repair DNA, BRCA2 plays a role in maintaining the stability of a cell's genetic information. Gene NRXN1 (neurexin 1) is among the largest known in human, molecular location on chromosome 2: base pairs 50,145,642 to 51,259,673. NRXN1 gene represents a strong candidate for involvement in the etiology of nicotine dependence, and even subtle changes in NRXN1 might contribute to susceptibility to autism.

We show in Figs 3 and 4 results for the T-dominated sub-sequences, whereas the results for A, C, and G-dominated sub-sequences are similar to those shown in the Figs. 3 and 4 (for each gene respectively). Fig. 3 shows (in the log-log scales) dependence of the standard deviation of the running density fluctuations $\langle \delta n(\tau)^2 \rangle^{1/2}$ on τ for the T-dominated subsequence of gene BRCA2. The straight line is drawn in this figure to indicate the scaling (2). The slope of this straight line provides us with the cluster-exponent $\alpha = 0.30 \pm 0.02$. Figure 4 shows analogous result for gene NRXN1 with $\alpha = 0.35 \pm 0.02$. One can see that in both cases we have rather strong cluster-

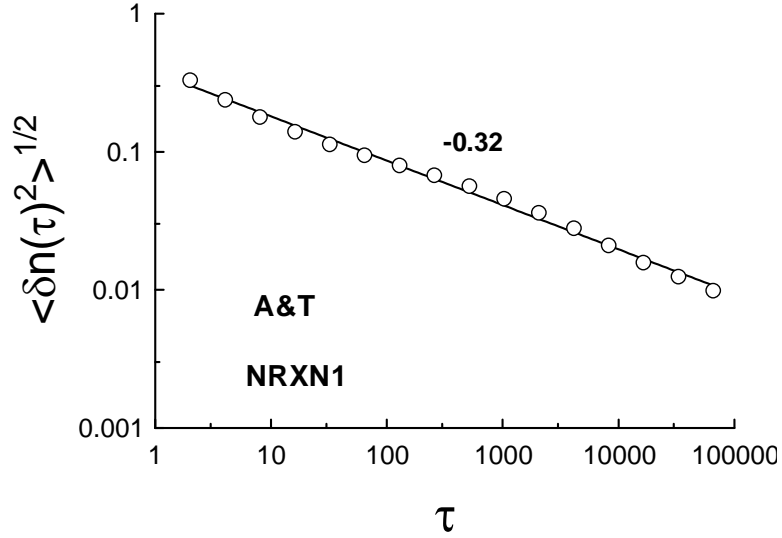


Figure 5: The standard deviation for $\delta n(\tau)$ vs τ for A& T (circles) dominated sub-sequence of gene NRXN1 (in log-log scales). The straight lines (the best fit) indicate the scaling law Eq. (2).

scaling with the cluster-exponent different for the different genes. The main consequence of the finite-size effects for the cluster-scaling is a wavy character of the scaling data in the log-log scales (cf. Ref. [14]).

3 Hydrogen bonds

The most popular potential for modeling the hydrogen (H) bond within a base-pair in the DNA chains is the Morse potential (see, for instance, Refs. [25],[26],[27],[28]):

$$V_i(y_i) = D_i \left[\exp - \left(\frac{a}{2} y_i \right) - 1 \right]^2 \quad (3)$$

where D_i is the site-dependent dissociation energy of the i th pair, which can take two values $D_i = D^{A-T}$ and $D_i = D^{C-G}$ for the A-T and the C-G pairs in the i th site respectively (the A-T pair includes two H bonds, while the C-G pair includes three H bonds, see Introduction); a^{-1} is a measure of the potential well width; variable y_i is a dynamical deviation of the H bonds from their equilibrium lengths at position i . The ratio $D^{C-G}/D^{A-T} = 1.5$ is often

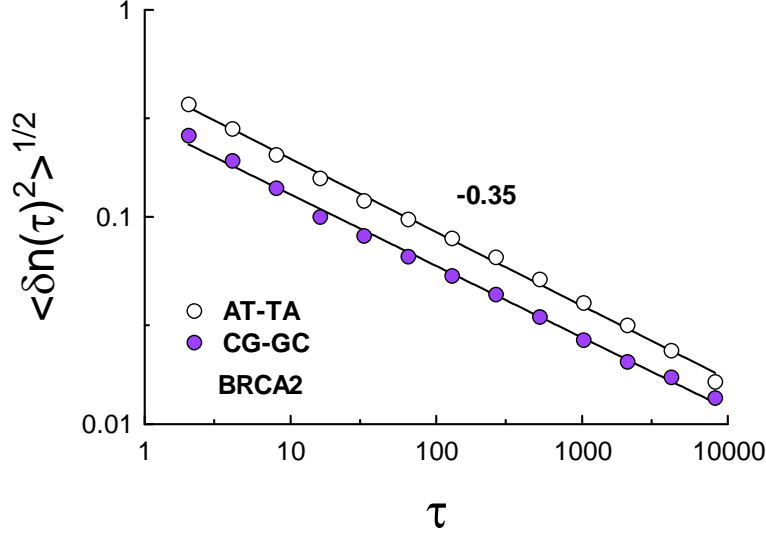


Figure 6: The standard deviation for $\delta n(\tau)$ vs τ for AT-TA (circles) and CG-GC (filled circles) dominated sub-sequence of gene BRCA2 (in log-log scales). The straight lines (the best fit) indicate the scaling law Eq. (2).

used for the model purposes (though recent quantum chemical calculations [29] results in a ratio $D^{C-G}/D^{A-T} = 2$).

Randomly distributed along the DNA chain bivalued H-bond coupling strengths D^{A-T} and D^{G-C} are usually used in the DNA dynamics models. This would be appropriate for an arbitrary base pair sequence. However, as it follows from previous consideration, homogeneous random distribution is not realistic even for the most long genes like NRXN1 (see, for instance, Ref. [30]). The dynamic heterogeneous properties of DNA molecule was considered, for instance, as a reason for the so-called multi-step melting [31]. However, the assumption of a random and short-range (delta-) correlated sequence made in Ref. [31] do not result in the multi-step melting and only an additional assumption of an additional backbone stiffness due to the double-stranded conformation of DNA molecule allowed to the authors to observe a multi-step melting in their model. In the model suggested In Ref. [32] the sequence randomness considered as a quenched noise with finite sequence correlation length. In this approach regions dominated by A-T or, alternatively, by C-G pairs play significant role in the bubble (i.e. locally denaturated states) formation.

Taking into account the cluster-scaling of the DNA nucleotides is a natural

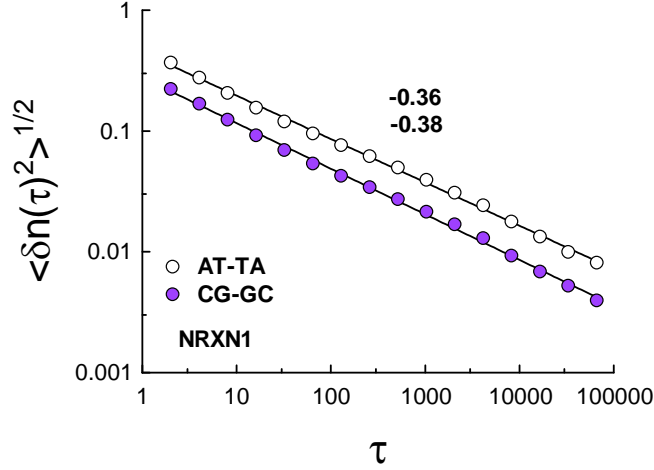


Figure 7: The standard deviation for $\delta n(\tau)$ vs τ for AT-TA (circles) and CG-GC (filled circles) dominated sub-sequence of gene NRXN1 (in log-log scales). The straight lines (the best fit) indicate the scaling law Eq. (2).

step toward more realistic dynamical model. Because of the bivalued H-bond coupling strengths: $D_i = D^{A-T}$ or $D_i = D^{G-C}$, this can be readily done using following bivalued mapping: $A = T = 1$, $C = G = 0$ or, alternatively, $C = G = 1$, $A = T = 0$. Figure 5 shows cluster-scaling behavior, Eq. (2), for the former mapping of NRXN1 gene. The cluster scaling exponent $\alpha = 0.32 \pm 0.02$ in this case. For $C = G = 1$, $A = T = 0$ the mapping calculations give the same result as well as for corresponding mappings of the gene BRCA2 (indication of an universality). Therefore, the bivalued sequences of the D_i coefficients for the DNA dynamic chain should be chosen as cluster-scaling ones with certain cluster-exponent α Eq. (2) (for the considered genes $\alpha \simeq 0.32$).

4 Stacking interaction

Two factors are mainly responsible for the stability of the DNA double helix: base pairing between complementary strands and stacking between adjacent bases (see Introduction). It is shown experimentally that DNA stability

is mainly determined by base-stacking interactions which contribute greatly into the dependence of the duplex stability on its sequence. (see, for instance, Ref. [1]). Therefore, it is interesting to check whether the stacking interactions dominate also the above-considered cluster-scaling phenomenon (cf. Introduction). In order to check this let us use following mapping: in combination $AT = TA = 1$, and $A = T = G = C = 0$ otherwise. An alternative mapping is: in combination $CG = GC = 1$, and $A = T = G = C = 0$ otherwise. If the stacking interactions dominate the cluster-scaling phenomenon, then one can expect that the cluster-scaling will be more pronounced just for these maps (cf. Fig. 1). It means that the cluster-exponent corresponding to these maps would be *smaller* than cluster-exponents observed for the above considered maps. As one can see comparing Figs. 6 and 7 with Figs. 3,4, and 5 in reality we have an opposite situation. This comparison indicates that the stacking interactions do not dominate the above-considered cluster-scaling phenomenon (at least for the examples given in the paper).

In a realistic dynamic model of DNA molecule one should take into account also the cluster-scaling of stacking interaction itself as it is shown in Figs. 6 and 7 for instance (see also Refs. [33],[34] for heterogeneity of both pairing and stacking interactions). This can be done in the frames of a commonly used approximation for the stacking potential (see, for instance, Ref. [35])

$$W_i(y_i, y_{i-1}) = \frac{\Delta H_i}{C} \left(1 - \exp \left(-b(y_i - y_{i-1})^2 \right) \right) \quad (4)$$

where ΔH_i can take different values for different stacked pairs $\{y_i, y_{i-1}\}$. Because the situation is not bivalued in this case this task seems to be more difficult than for the hydrogen bonds. The main problem here is hybridization of the nucleotides in different types of the stacked base-pairs (Fig. 1). The fact that the cluster-scaling exponents for the different types of stacked base-pairs have approximately the same value can help to solve this problem. This is not the case, however, for hybridization problem if one will consider a realistic model taking into account cluster-scaling of both hydrogen bonds and stacking interactions (the cluster-scaling exponents are different for hydrogen bonds: Fig. 5, and for stacking interactions: Figs. 6 and 7).

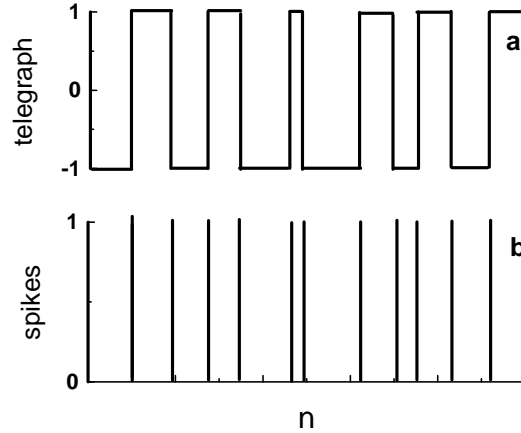


Figure 8: Mapping of a spiky sequence (figure 8b) into a telegraph one (figure 8a).

5 Chaotic order of the stacking interactions

Both stochastic and deterministic processes can result in the broad-band part of the spectrum, but the decay in the spectral power is different for the two cases. An exponential decay with respect to frequency refers to chaotic time series while a power-law decay indicates that the spectrum is stochastic. Not all chaotic systems have the exponentially decaying spectra, but appearance of an exponentially decaying spectrum in the system under consideration provides a strong indication that we have deal with a chaotic (deterministic) process [36]-[39]. The previously observed spectra of the DNA-sequences mappings exhibited power-law decay indicating a stochastic origin of the DNA-sequences randomness [18]-[24]. It should be noted that all the maps used in these investigations operated with simple use of the A or/and T or/and G or/and C numerical mapping. It seems, however, that a deeper insight in the underlying physics can be obtained using numerical maps operating with the combinations AT and TA which represent energy minima for the stacking interactions (cf. Fig. 1 and Ref. [15]). For this purpose we will put combinations $AT = TA = 1$, and $A = T = G = C = 0$ otherwise in a DNA-sequence under consideration (the multiple AT/TA combinations will be also considered as a single '1' in this mapping, for example: $ATATTA=1$). This map will represent a $\{0,1\}$ -values map of the stacking interactions energy minima sequence.

An additional technical problem will appear when one will try to analyze spectral properties of such map. The sequence will be very spiky and the

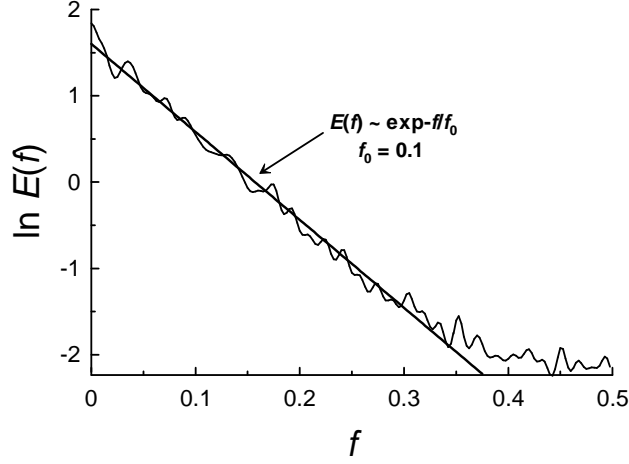


Figure 9: Spectrum of a telegraph series corresponding to the energy minima map constructed for the genome sequence of the *Arabidopsis thaliana*.

usual spectral methods (such as the fast Fourier transform or the maximum entropy method, for instance) will be practically useless. In order to solve this problem we will use an additional mapping of the spiky series into a telegraph signal. The spikes (symbols 1) are identical to each other and the dynamical information is coded in the length of the interspike intervals and the interspike intervals positions on the sequence, therefore it is the most direct way to map the spiky sequence into a telegraph signal, which has values -1 from one side of a spike and values +1 from another side of the spike. An example of such mapping is given in figure 8. While the dynamical information is here the same as for the corresponding spike sequence, the spectral methods are quite applicable to analysis of the telegraph series.

Figure 9 shows spectrum of a telegraph sequence corresponding to the above-described map constructed for the genome sequence of the *Arabidopsis thaliana*. We used the semi-log axes in the Fig. 9 in order to indicate exponential decay of the spectrum (the straight line). It should be noted that value of f_0 is not the same for different species (for human genome, for instance, $f_0 \simeq 0.05$).

Many of the well known chaotic attractors ('Lorenz', 'Rössler', etc.) exhibit the exponentially decaying spectra [37]. Here, for comparison with the Fig. 9, we will consider a chaotic spectrum generated by the Kaplan-Yorke map [40] (relevance of this choice will be clear immediately). In the Langevin

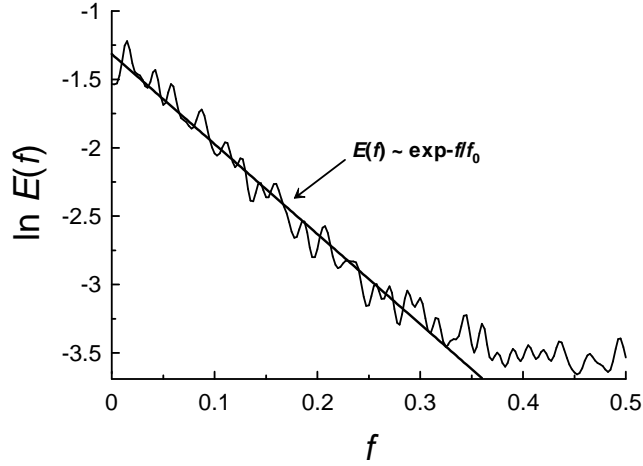


Figure 10: Spectrum of a chaotic solution of the Kaplan-Yorke map.

approach to Brownian motion the equation of motion is

$$\dot{y} = -\gamma y + F(t) \quad (5)$$

where the fluctuating kick force on the particle is a Gaussian white noise: $F(t) = \sum_n \eta_n \delta(t - n\tau)$ and $y(t)$ to take values in R^m . One can assume [41] that the evolution of the kick strengths is determined by a discrete time dynamical system T on the phase space and projected onto R^m by a function f :

$$\eta_n = f(x_{n-1}), \quad x_{n+1} = Tx_n \quad (6)$$

Then the solution of Eq. (5) is

$$y(t) = e^{-\gamma(t-n\tau)} y_n \quad (7)$$

where n equals the integer part of the relation t/τ and the recurrence

$$x_{n+1} = Tx_n, \quad y_{n+1} = \alpha y_n + f(x_n) \quad (8)$$

provides value of y_n (with $\alpha = e^{-\gamma\tau}$). In certain sense the dynamical system (8) is equivalent to the stochastic differential equation (5). In the generalization related to the Eq. (8) the force $F(t)$ can be considered as a *non*-Gaussian process which is determined by f and T . The Kaplan-Yorke map [40],[42],[43] is a particular simple case for this generalization:

$$Tx = 2x \pmod{1}, \quad f(x) = \cos 4\pi x \quad (9)$$

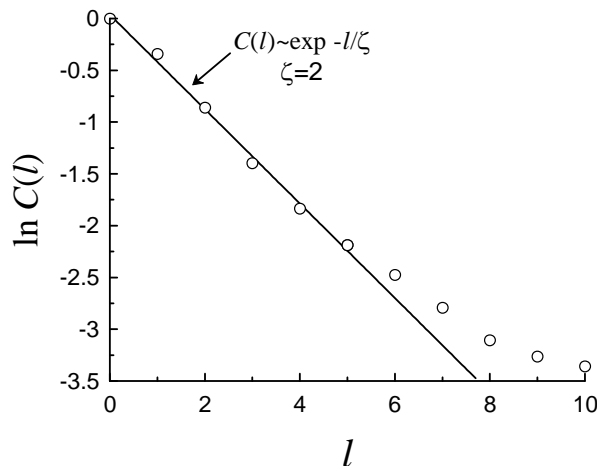


Figure 11: Autocorrelation function corresponding to the spectrum shown in Fig. 9.

Figure 10 shows spectrum of a chaotic solution of the Kaplan-Yorke map ($\alpha = 0.2$). We used the semi-log axes in this figure in order to indicate exponential decay of the spectrum (the straight line).

Although the exponential part of the spectrum in Fig. 9 is apparently extended to the frequencies $f \simeq 0.3$ for frequencies larger then $f \simeq 0.2$ (i.e. for scales $n \leq 5$) corresponding telegraph signal is a random one. This can be seen from the figure 11, which shows autocorrelation function corresponding to the spectrum shown in Fig. 9 (the correlation length $\zeta = 2$). We have a chaotic order on the large scales only (see also next section, Fig. 13). Fig. 12 shows analogous autocorrelation function for the Kaplan-Yorke solution.

6 Large-scale chaotic coherence

In the double-stranded DNA the two strands are complementary in a local sense, i.e. the nucleotide bases pair up such that A always pairs with T and G always pairs with C. But what can one say about nonlocal coherence of the nucleotides' sequences in the two strands? Actually, because of the local complimentary behavior this question can be answered by studying coherence between the A (map: A=1, T=C=G=0) and T (map: T=1, A=C=G=0) dominated sequences along a single strand (analogously for the C and G sequences). Due to the complementary properties of the A and T nucleotides the chaotic (deterministic) order of the energy minima of the

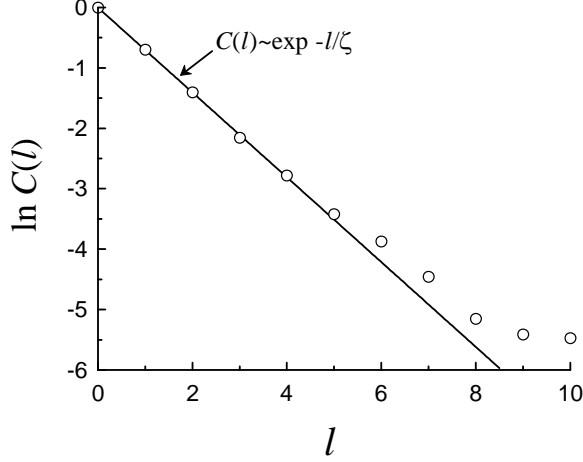


Figure 12: Autocorrelation function corresponding to the spectrum shown in Fig. 10.

stacking interactions should result in a large-scale coherence of the two DNA strands' sequences. This is mainly relevant to A and T sequences because just the AT/TA compositions correspond to the energy minima. Certain (however considerably smaller) large-scale coherence can appear also in C and G sequences as a secondary effect (see Fig. 13 and the explanations below). In order to compare coherent properties of the two DNA strands' sequences we will use cross-spectral analysis. The cross spectrum $E_{1,2}(f)$ of two processes $x_1(t)$ and $x_2(t)$ is defined by the Fourier transformation of the cross-correlation function normalized by the product of square root of the univariate power spectra $E_1(f)$ and $E_2(f)$:

$$E_{1,2}(f) = \frac{\sum_{\tau} \langle x_1(t)x_2(t-\tau) \rangle \exp(-i2\pi f\tau)}{2\pi \sqrt{E_1(f)E_2(f)}} \quad (6)$$

the bracket $\langle \dots \rangle$ denotes the expectation value. The cross spectrum can be decomposed into the phase spectrum $\phi_{1,2}(f)$ and the coherency $C_{1,2}(f)$:

$$E_{1,2}(f) = C_{1,2}(f)e^{-i\phi_{1,2}(f)} \quad (7)$$

Because of the normalization of the cross spectrum the coherency is ranging from $C_{1,2}(f) = 0$, i.e. no linear relationship between $x_1(t)$ and $x_2(t)$ at f , to $C_{1,2}(f) = 1$, i.e. perfect linear relationship.

Figure 13 shows coherency of the A (or T) dominated sequences on the two strands of the Arabidopsis DNA-duplex (solid curve), and coherency of

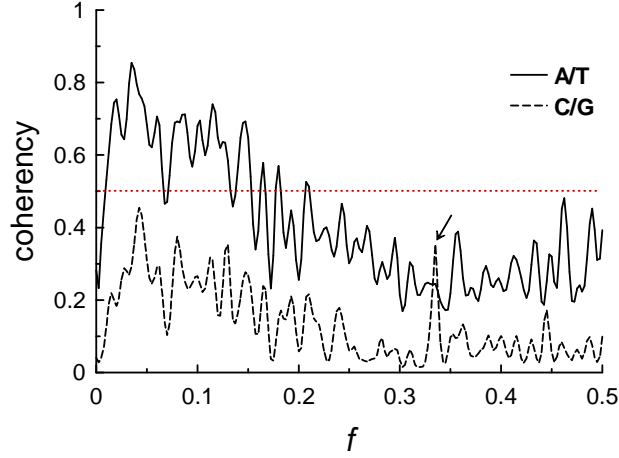


Figure 13: Coherency of the two DNA strands' sequences for the *Arabidopsis thaliana*.

the C (or G) dominated sequences (dashed curve). While the A (or T) dominated sequences exhibit rather high (> 0.5) coherency in a low-frequency domain $f < 0.15$ (i.e. for the length periods ≥ 7 nucleotides, cf. last paragraph of the previous Section), the C (or G) dominated sequences exhibit a low coherence even in this domain. The last (low) coherence is a secondary effect to the the former one (see above).

It should be also noted that the C/G coherency has a strong burst (the peak marked by an arrow in the Fig. 13) in a narrow vicinity of frequency $f \simeq 0.33$. This resonance peak comes from a very low coherency background and corresponds to the *codons'* period $T=3$ nucleotides ($T=1/f$). Let us recall that a codon is a sequence of three adjacent nucleotides constituting the genetic code (a specific amino acid residue in a polypeptide chain). Therefore, one can speculate that the two complimentary DNA strands can have relatively strong coherence related to the genetic code content in the case of the C/G containing codons, whereas the large-scale chaotic coherence related to the large-scale chaotic order in the A/T containing codons can suppress the genetic coherence (cf. Fig. 13). However, this speculation leads us beyond the pure physical frames of present paper.

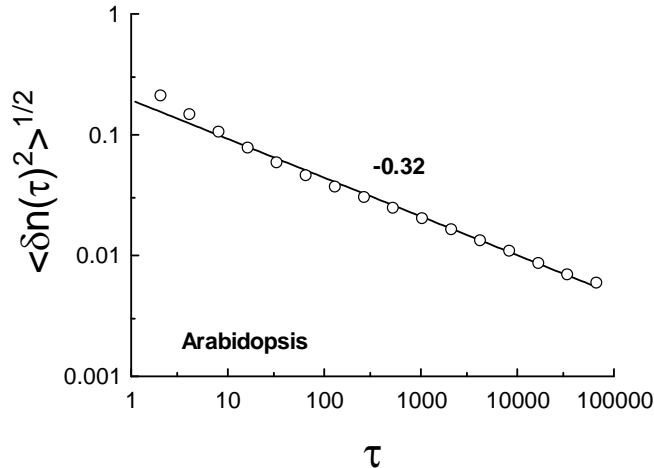


Figure 14: The standard deviation for $\delta n(\tau)$ vs. τ for the energy minima $\{0,1\}$ -map used in section V (in log-log scales). The straight lines (the best fit) indicate the scaling law Eq. (2).

7 Discussion

For the Gaussian-like processes there is a very close relationship between their spectral and cluster-scaling properties [15]. If the system under consideration is non-Gaussian, then this relationship is broken. The section V provides a good example of such situation. Indeed, figure 14 shows the standard deviation for $\delta n(\tau)$ vs. τ for the energy minima $\{0,1\}$ -mapping used in the section V. The straight lines (the best fit) indicate the scaling law Eq. (2). Thus, for the considered non-Gaussian system a robust cluster-scaling (Fig. 14) can co-exist with the non-scaling spectrum (Fig. 9). Therefore, the long-range correlations (which correspond to the power-law scaling spectra) in the human genome [18]-[23] are not directly related to its cluster-scaling properties. These two types of scaling behavior are independent for the non-Gaussian systems that makes the cluster-scaling method an independent tool for studying these systems. Moreover, while the previously used for the spectral computations simple maps indicate stochastic behavior, the intrinsic map for the energy minima of stacking interactions indicates a chaotic (deterministic) interactions in an underground of the stochastic system on large scales. This large-scale chaotic order can be operational in the resolving the random gap problem mentioned in the Introduction and should affect the DNA-duplex dynamics creating, in particular, the large-scale coherence between the two strands of the DNA-duplex.

References

- [1] Yakovchuk P., Protozanova E., and Frank-Kamenetskii M.D., *Nucleic Acids Research*, **34**, 564 (2006).
- [2] Saenger W., *Principles of Nucleic Acid Structure*, (Berlin: Springer, 1984).
- [3] Peyrard M., *Nonlinearity*, **17**, R1 (2004).
- [4] C. Vaillant, B. Audit, and A. Arneodo, *Phys. Rev. Lett.*, **99**, 218103 (2007).
- [5] Hyrien O., Marheineke K., Goldar A., *Bioessays* **25**, 116 (2003).
- [6] Jun S. and Rhind N., *Physics*, **1**, 32 (2008).
- [7] Blow, J. J., Gillespie, P. J., Francis, D., and Jackson, D. A., *J. Cell Biol.*, **15**, 15 (2001).
- [8] Rhind N., *Nat. Cell Biol.*, **8**, 1313 (2006).
- [9] Conti C., Sacc B. Herrick J., Lalou C., Pommier Y., and Bensimon A., *Mol. Biol. Cell.*, **18**: 3059 (2007).
- [10] Yang S. C-H., and Bechhoefer J., 2008, *Phys. Rev. E*, **78**, 041917 (2008).
- [11] Mesner, L. D., Li, X., Dijkwel, P. A., and Hamlin, J. L., *Mol. Cell. Biol.*, **23**, 804 (2003).
- [12] Shechter, D., and Gautier, J., *Cell Cycle* **4**, 235 (2005).
- [13] Stanley H.E., Buldyreva S.V., Goldbergerb A.L., Havlin S., Penga C-K., and Simons M., *Physica A*, **273**, 1 (1999).
- [14] Sreenivasan K.R., and Bershadskii A., *J. Stat. Phys.*, **125**, 1145 (2006).
- [15] A. Bershadskii, *Phys. Lett. A*, **360**, 210 (2006).
- [16] A. Bershadskii, *Phys. Lett. A*, **375**, 335 (2011).
- [17] D.W. Meinke, J.M. Cherry, C. Dean, et al., *Science*, **282**, 662 (1998).
- [18] Voss R.F., *Phys. Rev. Lett.*, **68**, 3805 (1992).

- [19] C.-K. Peng, S.V. Buldyrev, A.D. Goldberger, et al., *Nature*, **356** 168 (1992).
- [20] W. Li, and K. Kaneko, *Europhys. Lett.*, **17**, 655 (1992).
- [21] W. Li and D. Holste, *Phys. Rev. E*, **71**, 041910 (2005).
- [22] P. Carpena, P. Bernaola-Galvan, A. V. Coronado, et al., *Phys. Rev. E*, **75**, 032903 (2007).
- [23] Podobnik B., Shaoc J., Dokholyand N.V., Zlatice V., Stanley H.E., and Grosse I., *Physica A*, **373**, 497 (2007).
- [24] A. Arneodo, C. Vaillant, B. Audit et al., *Phys. Rep.*, **498**, 459 (2011).
- [25] Peyrard M., and Bishop A.R., *Phys. Rev. Lett.*, **62**, 2755 (1989).
- [26] Dauxois T., Peyrard M., and Bishop A.R., *Phys. Rev. E*, **47**, 684 (1993).
- [27] Campa A., and Giansanti A., *Phys. Rev. E*, **58**, 3585 (1998).
- [28] Hennig D., and Archilla J.F.R., *Phys. Scr.* **69**, 150 (2004).
- [29] Sponer, J., Leszczynski, J. and Hobza, P., *Biopolymers* **61**, 3 (2001).
- [30] Li W., Stolovitzky G., Bernaola-Galvan P., and Oliver J.L., *Genome Res.*, **8**, 916 (1998).
- [31] Cule D. and Hwa T., *Phys. Rev. Lett.*, **79**, 2375 (1997).
- [32] Jeon J-H., Park P-J., and Sung W, *J. Chem. Phys.*, **125**, 164901 (2007).
- [33] Ambjornsson T., Banik S.K., Krichevsky O., and Metzler R., *Phys. Rev. Lett.*, **97**, 128105 (2006).
- [34] Krueger A., Protozanova E., and Frank-Kamenetskii M.D., 2006, *Biophys. J.*, **90**, 3091
- [35] Joyeux M. and Florescu A-M., *J. Phys.: Condens. Matter*, **21**, 034101 (2009).
- [36] D.E. Sigeiti, *Phys. Rev. E*, **52**, 2443; *Physica D*, **82**, 136 (1995).

- [37] N. Ohtomo, K. Tokiwano, Y. Tanaka et. al., J. Phys. Soc. Jpn. **64** 1104 (1995).
- [38] J. D. Farmer, Physica D, **4**, 366 (1982).
- [39] U. Frisch and R. Morf, Phys. Rev., **23**, 2673 (1981).
- [40] J.L. Kaplan and J.A. Yorke, Lecture Notes in Mathematics, **730**, p. 204. (New York: Springer 1979).
- [41] C. Beck, Commun. Math. Phys., **130**, 51 (1990).
- [42] R.V. Jensen and C.R. Oberman, Phys. Rev. Lett., **46**, 1547 (1981).
- [43] J. C. Sprott, Chaos and Time-Series Analysis (Oxford-NY, Oxford Univ. Press, 2003)